Strong feedback limit of the Goodwin circadian oscillator

Aurore Woller and Didier Gonze
Université Libre de Bruxelles, Service de Chimie Physique, Campus Plaine, C.P. 231, 1050 Bruxelles, Belgium

Thomas Erneux
Université Libre de Bruxelles, Optique Nonlinéaire Théorique, Campus Plaine, C.P. 231, 1050 Bruxelles, Belgium

(Received 20 November 2012; published 29 March 2013)

The three-variable Goodwin model constitutes a prototypical oscillator based on a negative feedback loop. It was used as a minimal model for circadian oscillations. Other core models for circadian clocks are variants of the Goodwin model. The Goodwin oscillator also appears in many studies of coupled oscillator networks because of its relative simplicity compared to other biophysical models involving a large number of variables and parameters. Because the synchronization properties of Goodwin oscillators still remain difficult to explore mathematically, further simplifications of the Goodwin model have been sought. In this paper, we investigate the strong negative feedback limit of Goodwin equations by using asymptotic techniques. We find that Goodwin oscillations approach a sequence of decaying exponentials that can be described in terms of a single-variable leaky integrated-and-fire model.

DOI: 10.1103/PhysRevE.87.032722 PACS number(s): 87.18.Yt, 87.10.Ca, 87.18.Vf

I. INTRODUCTION

Strong negative autoregulation is prevalent in transcriptional networks to reduce gene expression heterogeneity [1] and metabolic costs of protein production [2], and to induce oscillatory gene expression [3]. It has also been suggested that negative feedback could be useful in signaling systems to increase information transmission [4]. A negative feedback also lies at the core of the molecular mechanism of circadian oscillators [5]. Its main structure is captured by the Goodwin model [6]. It is a minimal model that describes the oscillatory negative feedback regulation of a translated protein which indirectly inhibits its own transcription [7,8]. The Goodwin model is able both to oscillate with a 24 hour period and to reset its cycle with new light/dark patterns [9,10]. Modified versions of Goodwin model equations have been successfully used to describe the dynamics of the protein PER [11] which is known to play a crucial role in the circadian rhythms in fruit flies and mice [8], and for a circadian oscillating gene in the fungus *Neurospora crassa* [9,10].

In *Neurospora*, a strong resetting appears to be required to explain the experimental phase response curve and the short transients of the circadian oscillations after a perturbation [12]. A modified Goodwin model producing relaxation oscillations was shown to give results consistent with the experimental observation on *Neurospora* [10]. In contrast, such a strong resetting seems not present in higher organisms such as *Drosophila* and mammals [12]. As a core oscillator, the Goodwin model provides a means to explore a possible origin of relaxation oscillations.

An attractive feature of the Goodwin model is that it allows analytical studies of subtle dynamical phenomena, whereas other detailed biophysical models of cellular oscillators usually exhibit a large number of variables and parameters, which rule out any mathematical treatment, and obscure the underlying mechanisms. It is therefore not surprising that current investigations of the synchronization of cellular oscillators consider coupled Goodwin oscillator networks [13–15]. For large networks, it is desirable to reduce the Goodwin three-variable model to a single-variable fire-and-reset type model in order to benefit from the same computational efficiency as the coupled integrate-and-fire (IF) neurons used to simulate large scale brain models [16–19]. The main objective of this paper is to derive such IF model by using asymptotic techniques valid in the limit of strong negative feedbacks.

The Goodwin oscillator is described mathematically by the following three ordinary differential equations where X, Y, and Z denote the concentrations of mRNA, protein, and an inhibitor, respectively [7,8]:

$$X' = \frac{1}{1+Z^n} - kX, \tag{1}$$

$$Y' = X - kY, \tag{2}$$

$$Z' = Y - kZ. \tag{3}$$

Prime means differentiation with respect to time T. The sole source of nonlinearity comes from the negative feedback term in Eq. (1) which is the key biological mechanism raised by Goodwin. All the degradation constants have been taken equal to k because nearly equal constants favor the occurrence of limit-cycle oscillations [8]. The Goodwin model then depends on two parameters, namely, k and n.

Early theoretical work on the Goodwin family of oscillators was extensive but essentially devoted to the existence of periodic solutions [8,20]. Equations (1)–(3) admit a Hopf bifurcation at $k = k_H$ provided that n is sufficiently large ($n > 8$). The oscillations typically consist of a periodic sequence of successive (increasing and decreasing) exponentials. We wish to capture these functions analytically by investigating the large-n limit. In this limit, the feedback function approaches either 0 or 1 depending on the value of $Z - 1$. This does not mean that we may replace the feedback function in Eqs. (1)–(3) by the Heaviside step function $H(1 - Z)$. An important aspect of the large-n limit is the existence of fast time transition layers of size $\Delta T \sim n^{-1}$ that are connecting the two exponentials These layers are not present when the Heaviside function replaces the continuous feedback function

in Eq. (1). The Goodwin model with the Heaviside function has already been investigated by Tyson and Othmer [21] and by Tyson [22,23]. They derived a map relating the successive maxima of X and showed that a stable fixed point of the map corresponds to a limit-cycle solution of Goodwin equations. We revisit this problem with two objectives. First, we evaluate the numerical validity of this map by comparing bifurcation diagrams. We show that the approximation for the map fails near the Hopf bifurcation point, as expected since the oscillations are no more a combination of successive exponentials but are sinusoidal near the bifurcation point. Second, we investigate the small-k limit of the equations for the map and obtain analytical solutions of physical significance. We then derive two distinct IF models where all threshold values are determined analytically.

The plan of the paper is as follows. In Sec. II, we derive the equations for the map and test its validity by determining the bifurcation diagram. We also investigate the two fast transition layers and discuss their effects. In Sec. III, we investigate the small-k limit of the fixed point of the map and obtain simple expressions for the extrema and the period of the oscillations. This then leads to the formulation of single-variable IF type models. Last, we discuss in Sec. IV possible extensions of our analysis to periodically driven or coupled Goodwin oscillators.

II. STRONG NEGATIVE FEEDBACK

In this section, we analyze the limit-cycle solution of Eqs. (1)–(3) in the limit of large values of n keeping k fixed. For mathematical convenience, we reformulate Eqs. (1)–(3) in terms of $t = kT$, $x = k^{-2}X$, $y = k^{-1}Y$, $z = Z$ and find

$$x' = \frac{\alpha}{1+z^n} - x, \tag{4}$$

$$y' = x - y, \tag{5}$$

$$z' = y - z, \tag{6}$$

where prime now means differentiation with respect to time t and $\alpha \equiv k^{-3}$. The two parameters n and α now appear only in the first equation. A typical periodic solution for n large is shown in Fig. 1. The figure suggests that the extrema of x appear when $z = 1$ at times $t = 0$, s, and p. From now on, we define $t = 0$, s, and p as the times where $z = 1$. Because n is large, the negative feedback function in Eq. (4) periodically changes from 0 to α depending on the sign of $z - 1$. This motivates a two-part analysis of Eqs. (4)–(6). We first determine the solution when $z > 1$ ($0 < t < s$) and then the solution when $z < 1$ ($s < t < p$). The two solutions cannot exhibit discontinuities at time s and p and we will later investigate the transition layer problems.

A. Part $z > 1$

We start with the initial conditions $x(0) = x_0$, $y(0) = y_0$, and $z(0) = 1$ where the value of $x_0 > 1$ is assumed close to the maximum of x. Because $z > 1$ as time increases, we neglect the feedback function in Eqs. (4)–(6) and solve

$$x' = -x, \quad y' = x - y, \quad z' = y - z. \tag{7}$$

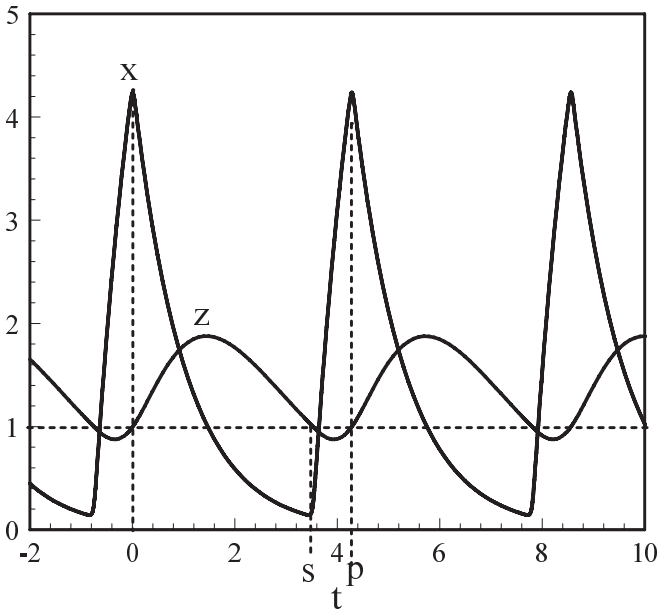

FIG. 1. Stable p-periodic solution of Eqs. (4)–(6) with $\alpha = 8$ and $n = 100$. The oscillations for x are a sequence of increasing and decreasing exponentials. The slow decrease occurs during the time interval s and the fast increase appears during the time interval $\Delta \equiv p - s$.

The solution of Eq. (7) is

$$x = x_0 \exp(-t), \tag{8}$$

$$y = \exp(-t)(y_0 + x_0 t), \tag{9}$$

$$z = \exp(-t)\left(1 + y_0 t + x_0 \frac{t^2}{2}\right). \tag{10}$$

At time $t = s$, we have $z = 1$, $x = x_1$, and $y = y_1$. From Eqs. (8)–(10), we determine the conditions

$$x_1 = x_0 \exp(-s), \tag{11}$$

$$y_1 = \exp(-s)(y_0 + x_0 s), \tag{12}$$

$$1 = \exp(-s)\left(1 + y_0 s + x_0 \frac{s^2}{2}\right). \tag{13}$$

B. Part $z < 1$

We next assume that $z < 1$ as $t > s$. The nonlinear function in Eq. (4) now equals α and we solve

$$x' = \alpha - x, \quad y' = x - y, \quad z' = y - z \tag{14}$$

with the initial conditions $x(s) = x_1$, $y(s) = y_1$, and $z(s) = 1$. The solution of Eq. (14) is

$$x = (x_1 - \alpha)\exp[-(t-s)] + \alpha, \tag{15}$$

$$y = \exp[-(t-s)]\,[y_1 - \alpha + (x_1 - \alpha)(t-s)] + \alpha, \tag{16}$$

$$1 = \exp[-(t-s)] \times \left[1 - \alpha + (y_1 - \alpha)(t-s) + (x_1 - \alpha)\frac{(t-s)^2}{2}\right] + \alpha. \tag{17}$$

Finally, we reenter the region $z > 1$ at time $t = p$. At this time, we have $z = 1$, $x = x_2$, and $y = y_2$. Using Eqs. (15)–(17), we find that x_2, y_2, and $\Delta \equiv p - s$ satisfy the conditions

$$x_2 = (x_1 - \alpha)\exp(-\Delta) + \alpha, \tag{18}$$

$$y_2 = \exp(-\Delta)\,[y_1 - \alpha + (x_1 - \alpha)\Delta] + \alpha, \tag{19}$$

$$1 = \exp(-\Delta)\left[1 - \alpha + (y_1 - \alpha)\Delta + (x_1 - \alpha)\frac{\Delta^2}{2}\right] + \alpha. \tag{20}$$

In summary, we determined equations for a map relating (x_2, y_2) and (x_0, y_0) defined as two successive maxima of x. The computation of (x_2, y_2) requires finding x_1, y_1, s, and Δ. Specifically, we start with (x_0, y_0) arbitrary and determine s from Eq. (13). We then evaluate (x_1, y_1) using Eqs. (11) and (12). With (x_1, y_1), we determine Δ from (20) and then (x_2, y_2) using Eqs. (18) and (19). We repeat this process until we approach a stable fixed point. The maximum and minimum of x are provided by x_0 and x_1, respectively.The period p is obtained by adding s and $\Delta = p - s$. The numerical bifurcation diagram obtained by solving numerically Eqs. (4)–(6) is compared to the numerical solution obtained by determining the fixed point of Eqs. (11)–(13) and Eqs. (18)–(20) (see Fig. 2). As $\alpha - 1 \to 0^+$, we note that the approximation provided by the map becomes singular ($p \to \infty$). Specifically, an analysis of this limit, detailed in Appendix A, indicates that

$$s = \sqrt{6(\alpha - 1)} \quad \text{and} \quad \Delta = -\ln(\alpha - 1) \to \infty \quad \text{as} \quad \alpha - 1 \to 0^+. \tag{21}$$

C. Transition layers

We analyze the transition layer near $t = s$ in detail and then summarize the main result for the layer near $t = p$. In order to analyze the solution near $t = s$, we introduce the inner variables [24]

$$x = x_1 + n^{-1}u, \quad y = y_1 + n^{-1}v, \quad z = 1 + n^{-1}w, \quad \text{and} \quad \tau = n(t - s), \tag{22}$$

where x_1 and y_1 are defined by (11) and (12), and s is the solution of Eq. (13). We note that

$$z^n = (1 + n^{-1}w)^n = \exp(w) + O(n^{-1}) \tag{23}$$

and rewrite Eqs. (4)–(6) in terms of u, v, w, and τ. We find

$$u' = \frac{\alpha}{1 + \exp(w) + O(n^{-1})} - x_1 + O(n^{-1}), \tag{24}$$

$$v' = x_1 - y_1 + O(n^{-1}), \tag{25}$$

$$w' = y_1 - 1 + O(n^{-1}), \tag{26}$$

where prime now means differentiation with respect to τ. The leading order equations as $n \to \infty$ with $v(0) = w(0) = 0$ can be solved analytically. We obtain

$$v = (x_1 - y_1)\tau, \quad w = (y_1 - 1)\tau, \tag{27}$$

$$u = -x_1\tau + \alpha\tau - \frac{\alpha}{y_1 - 1}\ln\{1 + \exp[(y_1 - 1)\tau]\}. \tag{28}$$

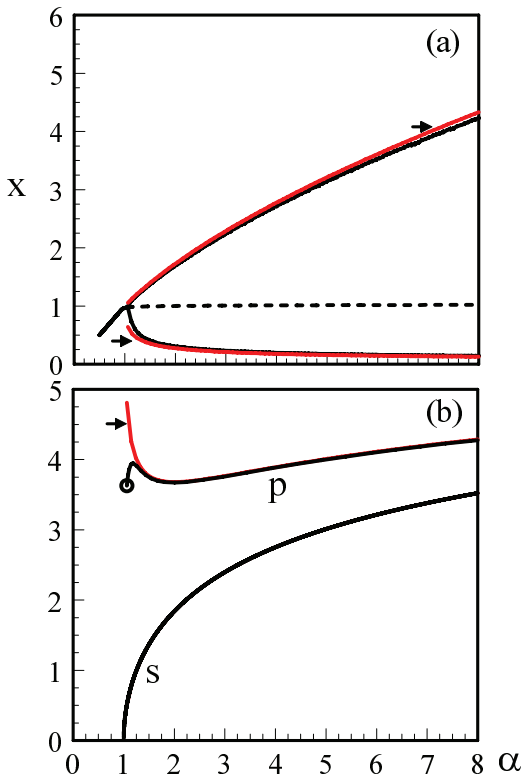

FIG. 2. (Color online) Bifurcation diagram of the steady and periodic solutions ($n = 100$). (a) The extrema of x obtained numerically from Eqs. (4)–(6) are shown as a function of α (black lines). They emerge from a Hopf bifurcation point located at $\alpha_H \sim 1$. The two lines indicated by arrows (red) are the extrema obtained by determining the stable fixed point of Eqs. (11)–(13) and Eqs. (18)–(20). (b) Period p of the oscillations and time s of the minimum of x. As $\alpha \to 1$, $p \to \infty$ meaning that the asymptotic approximation provided by the map (indicated by an arrow, red) fails near the Hopf bifurcation point. The dot at $\alpha = 1$ is the period of the oscillations at the Hopf bifurcation point given by $p = 2\pi/\sqrt{3}$. The period obtained numerically from Eqs. (4)–(6) exhibits a transition layer near $\alpha = 1$ before matching the approximation provided by the map. For s, the approximation provided by the map totally agrees with the numerically obtained value. Numerical simulations of Eqs. (4)–(6) have been realized using XPP-AUTO [25].

Note that $y_1 < 1$. The two limits of u as $\tau \to \pm\infty$ are $u \to (-x_1 + \alpha)\tau$ as $\tau \to \infty$ and $u \to -x_1\tau$ as $\tau \to -\infty$. We have verified that they are correctly matching the solutions described in the two previous subsections. The approximation (28) is shown in Fig. 3 and is in full agreement with the numerical solution. The figure shows that the minimum occurs before $\tau = 0$ where $z = 1$.

The transition layer solution near the maximum of the oscillations can be constructed in a similar way. The transition layer solution for $u \equiv n(x - x_0)$ as a function of $\tau \equiv n(t - p)$ is given by (28) with y_0 replacing y_1. We note that the maximum of the oscillations appears before $\tau = 0$ where $z = 1$.

III. INTEGRATE-AND-FIRE MODELS

A simple description of the response of an excitable cell to a stimulus is provided by the integrate-and-fire (IF)

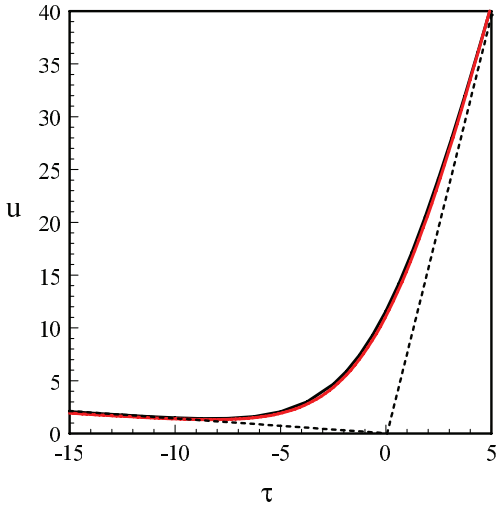

FIG. 3. (Color online) Transition layer near the minimum of x for $\alpha = 8$. The fixed point of the map is $x_0 = 4.33$, $x_1 = 0.13$, $y_0 = 1.70$, $y_1 = 0.50$, and $s = 3.52$. The approximation provided by (28) (red) is totally matching the solution of Goodwin equations (black, $\alpha = 8$ and $n = 100$). The two dotted straight lines are the limits $u = -x_1\tau$ as $\tau \to -\infty$ and $u = (\alpha - x_1)\tau$ as $\tau \to \infty$.

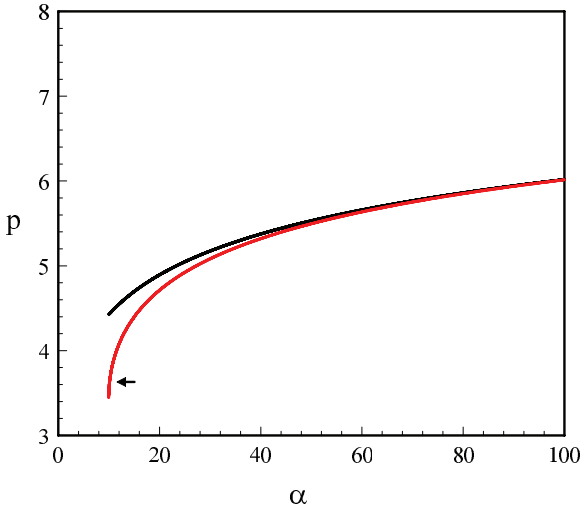

FIG. 4. (Color online) Period of the oscillations for α large. The solution obtained from the fixed point of the map (black line) is compared to its asymptotic approximation $p = s + \Delta$ using (32) and (33) ($3 < s < 6$, red line indicated by an arrow).

model [19]. In this model, the membrane potential $v(t)$ exhibits an exponential increase until the threshold $v = v_{\text{th}}$ is reached. The membrane potential "fires" and is immediately reset to zero. The equation describing the evolution of $v(t)$ is

$$\frac{dv}{dt} = -\frac{1}{\tau}v + c \tag{29}$$

and $v(t^+) = 0$ if $v(t) = v_{\text{th}}$, the threshold. The observation that Goodwin limit-cycle oscillations for n large can be built from exponential functions suggests that Goodwin equations could be replaced by linear equations similar to the IF model.

In Appendix B, we analyze the equations of the map in the limit $\alpha \to \infty$. The asymptotic solution for α large is best described in parametric form (with s as the parameter). Recall that the maxima (minima) of x and y are x_0 and y_0 (x_1 and y_1), respectively. Moreover, s is the time of the exponential decrease of x while $\Delta = p - s$ is the time of the exponential increase of x. In the large-s limit, we find the relations

$$x_0 = 2s^{-2}\exp(s), \quad x_1 = 2s^{-2}, \tag{30}$$

$$y_0 = 3 - 2s^{-1}, \quad y_1 = 2s^{-1}, \tag{31}$$

$$\Delta = \alpha^{-1/2}\sqrt{6(1 - 2s^{-1})}, \tag{32}$$

while $\alpha(s)$ is given by

$$\alpha = \frac{2}{3(1 - 2s^{-1})}[s^{-2}\exp(s)]^2. \tag{33}$$

By changing continuously s from a fixed value ($s > 2$), we may determine the extrema and the period. Figure 4 compares the period $p = s + \Delta$ obtained by using our analytical solution to the period obtained from the equations of the map.

Of physical interest are the leading approximations of the extrema of x and period p in terms of α. From (30)–(33), we find that

$$x_0 \simeq \sqrt{6\alpha}, \quad x_1 \simeq 0, \quad \text{and} \quad p \simeq \frac{1}{2}\ln\left(\frac{3\alpha}{2}\right) + \sqrt{\frac{6}{\alpha}}. \tag{34}$$

A change of parameter α will affect the maximum x_0 which scales as $\sqrt{\alpha}$ but not as much the period p which scales like $\ln(\alpha)$. We may now propose two different IF models that describe Goodwin spiking oscillations for α large (or k small).

A. One exponential

Neglecting the fast exponential increase, Goodwin oscillations approach a sequence of sawtooth oscillations which satisfy the equation

$$x' = -x \tag{35}$$

with the condition

$$x(t^+) = x_0 \quad \text{if} \quad x(t) = x_1. \tag{36}$$

According to our analysis this event appears at each multiple value of s. The values of s, x_0, and x_1 as a function of α are defined by (30) and (33).

B. Two exponentials

A more accurate IF model can be proposed if we take into account the fast exponential increase. Each time $x(t) = x_1$, we integrate

$$x' = -x + \alpha, \tag{37}$$

and when $x(t) = x_0 > x_1$, we integrate

$$x' = -x. \tag{38}$$

The oscillations described by the two IF models are shown in Fig. 5. Although both reduced models exhibit slightly higher maxima compared to the oscillations of the original Goodwin

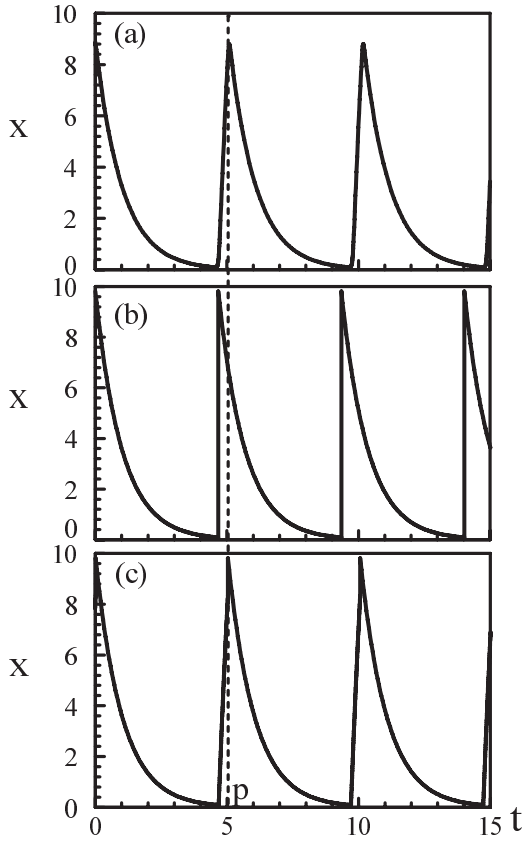

FIG. 5. Goodwin oscillations and its two approximations. The values of the parameters are $n = 75$ and $\alpha = 28$ (implying $x_0 = 9.81$ and $s = 4.67$). (a) Periodic solution of Goodwin equations (4)–(6). (b) One-exponential approximation using Eqs. (35) and (36). (c) Two-exponential approximation that includes the fast exponential increase using sequentially Eqs. (37) and (38).

equations, the period p of the oscillations is quantitatively captured by the second IF model.

IV. DISCUSSION

The Goodwin model constitutes a prototypical oscillator based on a negative feedback loop. It was used as a minimal model for circadian oscillations [9,10]. Other core models for circadian clocks are variants of the Goodwin model [11,13–24,26,27]. The Goodwin model was also used to model the ultradian Hes1 oscillations controlling the somitogenesis [28].

Thus, understanding the dynamical properties of such a generic model is of high interest in deciphering the design principles of biological oscillators [29]. Early theoretical works on the Goodwin model were devoted to prove the existence of limit cycle oscillations [20,30]. Subsequent works have proposed variants and extensions of the Goodwin model in search of processes favoring the oscillations. Those include nonlinear reaction rates [31], time delay through multiple reaction steps [21], feedback inhibition [32], and explicit gene-protein binding/unbinding dynamics [33].

In the present work, we have derived an analytical solution for the Goodwin model in the limit of strong feedback (n large). The solution for the limit cycle is expressed as a combination of exponential functions and resembles relaxation oscillations. The limit case where the inhibition is treated as a step function was already considered by Tyson [22] and further commented on by Painter and Bliss [34]. Compared to these earlier works, we have analyzed the numerical validity of all approximations in terms of bifurcation diagrams for the extrema and the period of the oscillations. Mathematically, we examined specific limits of the control parameter and we also discussed the role of fast transition layers. Ruoff *et al*. [10,35] have artificially obtained similar relaxation-like oscillations by replacing the Hill inhibitory function with a "resetting function" that abruptly changes from 0 (inhibition) to 1 (no inhibition) when the variable z passes through threshold values. Interestingly, we do not need to assume such an artificial resetting function or additional positive feedback loops (which generate different time scales in the system) to get relaxation-like oscillations.

Although a high Hill exponent cannot be justified by simple cooperative regulatory processes, our results suggest that the nature and steepness of the negative feedback regulation may play an important role in the shape of the oscillations and, presumably, in its entrainment and phase shifting performances. The abruptness of the resetting of the oscillations appears to differ from one organism to another. In *Neurospora*, a strong resetting seems to be required to explain the experimental phase response curve whereas in *Drosophila*, the resetting seems more soft [12]. This can be of importance for a proper adaptation of the organisms. Our results suggest that, besides other interconnected feedback loops [36], the strength of feedback regulation is a critical way to control the oscillator features.

The success of our analysis in deriving simple expressions for the limit-cycle oscillations motivates the study of other problems of interest in the circadian oscillator community. We wish to investigate the case of coupled Goodwin oscillators and verify that the strong feedback limit indeed leads to coupled IF oscillators. Another problem is the strong feedback limit of a periodically driven Goodwin oscillator. The derivation of reduced models will obviously depend on how we couple Goodwin oscillators or on how the modulation is introduced in Goodwin equations.

ACKNOWLEDGMENTS

The work of D.G. is supported by Grant No. 3.4636.04 from the Fonds de la Recherche Scientifique Médicale (F.R.S.M., Belgium). T.E. acknowledges the support of the Fonds National de la Recherche Scientifique (Belgium).

APPENDIX A: THE LIMIT $\alpha - 1 \to 0^+$

With $x_2 = x_0$ and $y_2 = y_0$ in Eqs. (18) and (19), Eqs. (11)–(13) and (18)–(20) for the fixed point of the map are given by

$$x_1 = x_0 \exp(-s), \tag{A1}$$

$$y_1 = \exp(-s)(y_0 + x_0 s), \tag{A2}$$

$$1 = \exp(-s)\left(1 + y_0 s + x_0 \frac{s^2}{2}\right), \tag{A3}$$

$$x_0 = (x_1 - \alpha)\exp(-\Delta) + \alpha, \tag{A4}$$

$$y_0 = \exp(-\Delta)\,[y_1 - \alpha + (x_1 - \alpha)\Delta] + \alpha, \tag{A5}$$

$$1 = \exp(-\Delta)\left[1 - \alpha + (y_1 - \alpha)\Delta + (x_1 - \alpha)\frac{\Delta^2}{2}\right] + \alpha. \tag{A6}$$

Equations (A1)–(A6) are six transcendental equations for the six unknowns x_0, x_1, y_0, y_1, s, and Δ and we are interested in finding their limits as $\alpha - 1 \to 0^+$.To this end, we first eliminate x_1 and y_1: From Eqs. (A4) and (A5), we extract x_1 and y_1 as

$$x_1 = \alpha + (x_0 - \alpha)\exp(\Delta), \tag{A7}$$

$$y_1 = \alpha + (y_0 - \alpha)\exp(\Delta) - \Delta(x_0 - \alpha)\exp(\Delta). \tag{A8}$$

Inserting then (A7) and (A8) into Eqs. (A1), (A2), and (A6), our problem reduces to the following four equations for x_0, y_0, s, and Δ:

$$\alpha + (x_0 - \alpha)\exp(\Delta) = x_0\exp(-s), \tag{A9}$$

$$[\alpha + (y_0 - \alpha)\exp(\Delta) - \Delta(x_0 - \alpha)\exp(\Delta)] = \exp(-s)(y_0 + x_0 s), \tag{A10}$$

$$[1 - \exp(-s)] = \exp(-s)\left(y_0 s + x_0\frac{s^2}{2}\right), \tag{A11}$$

$$(1-\alpha)[1 - \exp(-\Delta)] = \Delta\left[y_0 - \alpha - \frac{\Delta}{2}(x_0 - \alpha)\right]. \tag{A12}$$

A simple expression for x_0 can be found from Eq. (A9) and is given by

$$x_0 = \frac{\alpha[1 - \exp(\Delta)]}{\exp(-s) - \exp(-\Delta)} = \frac{\alpha}{1 + \frac{1-\exp(-s)}{\exp(\Delta)-1}}. \tag{A13}$$

The last expression in Eq. (A13) will be useful when we investigate the double limit $s \to 0$ and $\Delta \to \infty$. From Eq. (A11), we next determine y_0 in terms of s and x_0. We find

$$y_0 = \frac{\exp(s) - 1 - x_0\frac{s^2}{2}}{s}. \tag{A14}$$

Using (A13) and (A14), we may eliminate x_0 and y_0 in the remaining equations (A10) and (A12). Our problem then consists of two equations for s and Δ.

We are now ready to explore the limit $\alpha - 1 \to 0^+$. Numerically, we note that $s \to 0$ and $\Delta \to \infty$ in this limit. We anticipate our final results by assuming the following scalings for s and $\exp(-\Delta)$:

$$s \sim (\alpha - 1)^{1/2} \quad \text{and} \quad \exp(-\Delta) \sim \frac{\alpha - 1}{\Delta^2 s}. \tag{A15}$$

Starting with Eqs. (A13) and (A14), we first note that

$$x_0 \simeq \alpha - \alpha s\exp(-\Delta), \tag{A16}$$

$$y_0 \simeq 1 + \frac{s^2}{6}, \tag{A17}$$

where we have kept the leading term and its first correction. The correction terms are needed because the expressions $x_0 - \alpha$ and $y_0 - \alpha = y_0 - 1 - (\alpha - 1)$ appear in both Eqs. (A10) and (A12).

Substituting (A16) and (A17) into Eq. (A10), we obtain

$$\alpha + \left(1 + \frac{s^2}{6} - \alpha\right)\exp(\Delta) + \Delta s = 1 - \frac{s^2}{3} + \cdots, \tag{A18}$$

or equivalently,

$$\left(1 + \frac{s^2}{6} - \alpha\right)\exp(\Delta) + \Delta s = 1 - \alpha - \frac{s^2}{3}. \tag{A19}$$

Multiplying both sides by $\exp(-\Delta)$ we find

$$\left(1 + \frac{s^2}{6} - \alpha\right) + \Delta s\exp(-\Delta) = \exp(-\Delta)\left(1 - \alpha - \frac{s^2}{3}\right). \tag{A20}$$

The term in parentheses on the left-hand side of Eq. (A20) is proportional to $1 - \alpha$ since $s \sim (\alpha - 1)^{1/2}$. The second term on the left-hand side is proportional to $(\alpha - 1)/\Delta$ after we eliminate $\exp(-\Delta)$ using (A15). Similarly, we note that the expression on the right-hand side is proportional to $(\alpha - 1)^{3/2}/\Delta^2$ We conclude that the first and second terms on the left-hand side represent the leading contribution and its first correction, respectively. Neglecting the right-hand side, we have

$$\left[1 - \alpha + \frac{s^2}{6}\right] = -\Delta s\exp(-\Delta). \tag{A21}$$

We next substitute (A16) and (A17) into Eq. (A12) and obtain

$$(1 - \alpha) = \Delta\left(1 + \frac{s^2}{6} - \alpha + \frac{\Delta}{2}s\exp(-\Delta)\right), \tag{A22}$$

where we have neglected terms proportional to $(\alpha - 1)$ $\exp(-\Delta)$ and $\Delta(\alpha - 1)^{3/2}$. We divide Eq. (A22) by Δ and find

$$\left[1 - \alpha + \frac{s^2}{6}\right] = \frac{(1 - \alpha)}{\Delta} - \frac{\Delta}{2}s\exp(-\Delta). \tag{A23}$$

The left-hand side is proportional to $\alpha - 1$. The two terms on the right-hand side are both proportional to $(\alpha - 1)/\Delta$ which is smaller in size than the left-hand side. The leading solution for both Eqs. (A21) and (A23) is given by the same left-hand side and we determine s as

$$s = \sqrt{6(\alpha - 1)}. \tag{A24}$$

By subtracting Eqs. (A21) and (A23), we obtain

$$-\frac{\Delta}{2}s\exp(-\Delta) + \frac{(\alpha - 1)}{\Delta} = 0, \tag{A25}$$

or after using (A24), the implicit solution

$$\alpha - 1 = \tfrac{3}{2}\Delta^4\exp(-2\Delta), \tag{A26}$$

which implies that $\Delta = -\frac{1}{2}\ln(\alpha - 1) \to \infty$ as $\alpha - 1 \to 0^+$.

APPENDIX B: THE LIMIT $\alpha \to \infty$

We consider Eqs. (A9)–(A12) for the four unknowns x_0, y_0, s, and Δ. We need to compare $\exp(-s)$ small to quantities that are proportional to rational powers of α. To this end, we introduce a new parameter $r = r(\alpha)$ defined by

$$r \equiv s^2 x_0\exp(-s). \tag{B1}$$

This definition is motivated by the structure of Eq. (A11). Assuming

$$y_0 = O(1), \quad x_0 = O(\alpha^{1/2}), \quad \text{and} \quad s = O(\ln(\alpha)), \tag{B2}$$

Eq. (A11) reduces to

$$1 = \exp(-s)x_0\frac{s^2}{2} \tag{B3}$$

and implies that

$$r = 2, \tag{B4}$$

in first approximation. We next analyze the remaining equations assuming the scalings (B2) and

$$\Delta = O(\alpha^{-1/2}). \tag{B5}$$

We start with Eq. (A9). After simplifying one α, we find

$$x_0 + (x_0 - \alpha)\Delta + (x_0 - \alpha)\frac{\Delta^2}{2} + \cdots = 2s^{-2}. \tag{B6}$$

The leading order problem is $O(\alpha^{1/2})$ and gives $x_0 = \alpha\Delta$. However, we shall need the next correction term for the analysis of Eq. (A10). Two successive iterations of Eq. (B6) lead to the expression

$$x_0 = \alpha\Delta - \frac{\alpha\Delta^2}{2}. \tag{B7}$$

We consider Eq. (A10). We first expand $\exp(\Delta)$, simplify one α, one $\alpha\Delta$, and obtain

$$-\frac{\alpha\Delta^2}{2} + \cdots + y_0(1 + \cdots) - \Delta x_0(1 + \cdots) + \Delta\alpha(\Delta + \cdots) = 2\left(\frac{1}{s} + \cdots\right), \tag{B8}$$

where the dots refer to higher order corrections terms in either Δ or s^{-1}. We eliminate x_0 by introducing (B7) into (B8) and simplify one $\alpha\Delta^2$. We then obtain an expression for y_0 given by

$$y_0 = \frac{\alpha}{2}\Delta^2 + \frac{2}{s}. \tag{B9}$$

Finally, we expand $\exp(\Delta)$ in Eq. (A12) and use (B7), and (B9):

$$\begin{aligned}(1-\alpha)[1 - (1 - \Delta + \Delta^2/2 - \Delta^3/6 + \cdots)] &= \Delta\left[\frac{\alpha}{2}\Delta^2 + \frac{2}{s} - \alpha - \frac{\Delta}{2}\left(\alpha\Delta - \frac{\alpha\Delta^2}{2} - \alpha\right)\right],\\ (\Delta + \cdots) - \alpha(\Delta - \Delta^2/2 + \Delta^3/6 + \cdots) &= \Delta\left[\frac{\alpha}{2}\Delta^2 + \frac{2}{s} - \alpha - \frac{\Delta}{2}\left(\alpha\Delta - \frac{\alpha\Delta^2}{2} - \alpha\right)\right].\end{aligned} \tag{B10}$$

Simplifying $\alpha\Delta^2/2$ in the square brackets, and then simplifying one $\alpha\Delta$ and one $\alpha\Delta^2/2$ on both the left- and right-hand sides, Eq. (B10) reduces to

$$(\Delta + \cdots) - \alpha(\Delta^3/6 + \cdots) = \Delta\left[\frac{2}{s} - \frac{\Delta}{2}\left(-\frac{\alpha\Delta^2}{2}\right)\right]. \tag{B11}$$

The dominant contribution in Eq. (B11) is $O(\alpha^{-1/2})$ and leads to an expression for Δ given by

$$\Delta = \sqrt{\frac{6}{\alpha}\left(1 - \frac{2}{s}\right)}. \tag{B12}$$

Using (A1) and (A2), we find that x_1 and y_1 are small like

$$x_1 = 2s^{-2} \quad \text{and} \quad y_1 = 2s^{-1}. \tag{B13}$$

The large-α limit is best described in parametric form using large s as a parameter. The time Δ is given by (B12). Inserting (B12) into Eqs. (B7) and (B9), we determine x_0 and y_0 as

$$x_0 = \alpha^{1/2}\sqrt{6\left(1 - \frac{2}{s}\right)} - 3\left(1 - \frac{2}{s}\right), \tag{B14}$$

$$y_0 = 3 - \frac{4}{s}. \tag{B15}$$

Equation (B1) with (B4) provides another expression for x_0 given by

$$x_0 = \frac{2}{s^2}\exp(s). \tag{B16}$$

Inserting (B16) into (B14) then leads to the following expression for $\alpha = \alpha(s)$:

$$\alpha = \frac{2}{3\left(1 - \frac{2}{s}\right)}\left[\frac{1}{s^2}\exp(s)\right]^2. \tag{B17}$$

Finally, the period of the oscillations is given by $p = s + \Delta$.

[1] A. Becskei and L. Serrano, Nature (London) **405**, 590 (2000).
[2] D. J. Stekel and D. J. Jenkins, BMC Syst. Biol. **2**, 6 (2008).
[3] M. B. Elowitz and S. Leibler, Nature (London) **403**, 335 (2000).
[4] R. C. Yu, C. G. Pesce, A. Colman-Lerner, L. Lok, D. Pincus, E. Serra, M. Holl, K. Benjamin, A. Gordon, and R. Brent, Nature (London) **456**, 755 (2008).
[5] M. W. Young and S. A. Kay, Nat. Rev. Genet. **2**, 702 (2001).
[6] B. Goodwin, Adv. Enzyme Regul. **3**, 425 (1965).
[7] J. D. Murray, *Mathematical Biology I: An Introduction*, 3rd ed. (Springer, New York, 2002), Chap. 7.
[8] *Computational Cell Biology*, edited by C. P. Fall, E. S. Marland, J. M. Wagner, and J. J. Tyson, Interdisciplinary Applied Mathematics, Vol. 20 (Springer, New York, 2002), Chap. 9.
[9] P. Ruoff, M. Vinsjevik, C. Monnerjahn, and L. Rensing, J. Biol. Rhythms **14**, 469 (1999).

[10] P. Ruoff, M. Vinsjevik, C. Monnerjahn, and L. Rensing, J. Theor. Biol. **209**, 29 (2001).
[11] A. Goldbeter, Proc. Biol. Sci. **261**, 319 (1995).
[12] L. Rensing, U. Meyer-Grahle, and P. Ruoff, Chronobiol. Int. **18**, 329 (2001).
[13] D. Gonze, S. Bernard, C. Waltermann, A. Kramer, and H. Herzel, Biophys. J. **89**, 120 (2005).
[14] N. Komin, A. C. Murza, E. Hernández-García, and R. Toral, Interface Focus **1**, 167 (2011).
[15] E. Ullner, J. Buceta, A. Diez-Noguera, and J. Garcia-Ojalvo, Biophys. J. **96**, 3573 (2009).
[16] G. B. Ermentrout and D. H. Terman, *Mathematical Foundations of Neuroscience* (Springer, New York, 2010).
[17] D. Hansel, G. Mato, C. Meunier, and L. Neltner, Neural Comput. **10**, 467 (1998).
[18] E. M. Izhikevich and G. M. Edelman, Proc. Natl. Acad. Sci. USA **105**, 3593 (2008).
[19] S. Coombes, R. Thul, and K. C. A. Wedgwood, Physica D **241**, 2042 (2012).
[20] J. S. Griffith, J. Theor. Biol. **20**, 202 (1968).
[21] J. J. Tyson and H. G. Othmer, Prog. Theor. Biol. **5**, 1 (1978).
[22] J. J. Tyson, J. Theor. Biol. **80**, 27 (1979).
[23] J. J. Tyson, J. Theor. Biol. **103**, 313 (1983).
[24] C. M. Bender and S. A. Orszag, *Advanced Mathematical Methods for Scientists and Engineers* (McGraw Hill, New York, 1978).
[25] B. Ermentrout, *Simulating, Analyzing, and Animating Dynamical Systems: A Guide to XPPAUT for Researchers and Students* (SIAM, Philadelphia, 2002).
[26] D. Gonze and A. Goldbeter, J. Stat. Phys. **101**, 649 (2000).
[27] C. Gérard, D. Gonze, and A. Goldbeter, Philos. Trans. R. Soc., A **367**, 4665 (2009).
[28] S. Zeiser, J. Müller, and V. Liebscher, J. Comput. Biol. **14**, 984 (2007).
[29] B. Novak and J. J. Tyson, Nat. Rev. Mol. Cell Biol. **9**, 981 (2008).
[30] J. D. Allwright, J. Math. Biol. **4**, 363 (1977).
[31] C. F. Walter, J. Theor. Biol. **44**, 219 (1974).
[32] R. D. Bliss, P. R. Painter, and A. G. Marr, J. Theor. Biol. **97**, 177 (1982).
[33] P. E. Morant, Q. Thommen, F. Lemaire, C. Vandermoere, B. Parent, and M. Lefranc, Phys. Rev. Lett. **102**, 068104 (2009).
[34] P. R. Painter and R. D. Bliss, J. Theor. Biol. **90**, 293 (1981).
[35] P. Ruoff, J. J. Loros, and J. C. Dunlap, Proc. Natl. Acad. Sci. USA **102**, 17681 (2005).
[36] T. Saithong, K. J. Painter, and A. J. Millar, PLoS One **5**, e13867 (2010).